# Antifibrotic effect of xanthohumol in combination with praziquantel is associated with altered redox status and reduced iron accumulation during liver fluke-associated cholangiocarcinogenesis

**Wassana Jamnongkan** [1,2] , **Malinee Thanee** [1,2] , **Puangrat Yongvanit** [1,2] , **Watcharin Loilome** [1,2] , **Raynoo Thanan** [1,2] , **Phongsaran Kimawaha** [2,3] , **Tidarat Boonmars** [2,4] , **Runglawan Silakit** [1,2] , **Nisana Namwat** [1,2] , **Anchalee Techasen** [Corresp. 2,3]

1 Department of Biochemistry, Faculty of Medicine, Khon Kaen University, Khon Kaen, Thailand

2 Cholangiocarcinoma Research Institute, Khon Kaen University, Khon Kaen, Thailand

3 Faculty of Associated Medical Sciences, Khon Kaen University, Khon Kaen, Thailand

4 Department of Parasitology, Faculty of Medicine, Khon Kaen University, Khon Kaen, Thailand

Corresponding Author: Anchalee Techasen
Email address: anchte@kku.ac.th

Cholangiocarcinoma (CCA) caused by infection by the liver fluke *Opisthorchis viverrini*, (Ov) is the major public health problem in northeast Thailand. Following Ov infection the subsequent molecular changes can be associated by reactive oxygen species (ROS) induced chronic inflammation, advanced periductal fibrosis, and cholangiocarcinogenesis. Notably, resistance to an activation of cell death in prolonged oxidative stress conditions can occur but some damaged/mutated cells could survive and enable clonal expansion. Our study used a natural product, xanthohumol (XN) which is an anti-oxidant and anti-inflammatory compound to examine whether it could prevent Ov-associated CCA carcinogenesis. We measured the effect of XN with or without praziquantel (PZ), an anti-helminthic treatment, on DNA damage, redox status change including iron accumulation and periductal fibrosis during CCA genesis induced by administration of Ov and *N*-dinitrosomethylamine (NDMA) in hamsters. Animals were randomly divided into four groups: group I, Ov infection and NDMA administration (ON); group II, Ov infection and NDMA administration and PZ treatment (ONP); the latter 2 groups were similar to group I and II, but group III received additional XN (XON) and group IV received XN plus PZ (XONP). The results showed that high 8-oxodG (a marker of DNA damage) was observed throughout cholangiocarcinogenesis. Moreover, increased expression of CD44v8-10 (a cell surface in regulation of the ROS defense system), whereas decreased expression of phospho-p38$^{MAPK}$ (a major ROS target), was found during the progression of the bile duct cell transformation. In addition, high accumulation of iron and expression of transferrin receptor-1 (TfR-1) in both malignant bile ducts and inflammatory cells were detected.

Furthermore, fibrosis also increased with the highest level being on day 180. On the other hand, the groups of XN with or without PZ supplementations showed an effective reduction in all the markers examined, including fibrosis when compared with ON group. In particular, the XONP group in which a significant reduction DNA damage occured, was also found to have iron accumulation and fibrosis compared to the other groups. Our results show that XN administered in combination with PZ could efficiently prevent CCA development and hence provide potential chemopreventive benefits in Ov-induced cholangiocarcinogenesis.

1   **Antifibrotic effect of xanthohumol in combination with praziquantel is associated with**

2   **altered redox status and reduced iron accumulation during liver fluke-associated**

3   **cholangiocarcinogenesis**

4   Wassana Jamnongkan[1,4], Malinee Thanee[1,4],  Puangrat Yongvanit[1,4] , Watcharin Loilome[1,4],

5   Raynoo Thanan[1,4], Phongsaran Kimawaha[2,4], Tidarat Boonmars [3,4], Runglawan Silakit[1,4],  Nisana

6   Namwat[1,4] and Anchalee Techasen[2,4]*

7   [1]Departments of Biochemistry, [3]Parasitology, Faculty of Medicine, Khon Kaen University, Khon

8   Kaen, Thailand.

9   [2]Faculty of Associated Medical Sciences, Khon Kaen University, Khon Kaen, Thailand.

10   [4]Cholangiocarcinoma Research Institute, Khon Kaen University, Khon Kaen, Thailand.

11   **Address correspondence to:**

12   Dr. Anchalee Techasen

13   Faculty of Associated Medical Sciences, Khon Kaen University, Khon Kaen, Thailand. Phone

14   +66 43 202086, Telefax+66 43 202086

15   E-mail address:  anchte@kku.ac.th

**ABSTRACT**

Cholangiocarcinoma (CCA) caused by infection by the liver fluke *Opisthorchis viverrini*, (Ov) is the major public health problem in northeast Thailand. Following Ov infection the subsequent molecular changes can be associated by reactive oxygen species (ROS) induced chronic inflammation, advanced periductal fibrosis, and cholangiocarcinogenesis. Notably, resistance to an activation of cell death in prolonged oxidative stress conditions can occur but some damaged/mutated cells could survive and enable clonal expansion. Our study used a natural product, xanthohumol (XN) which is an anti-oxidant and anti-inflammatory compound to examine whether it could prevent Ov-associated CCA carcinogenesis. We measured the effect of XN with or without praziquantel (PZ), an anti-helminthic treatment, on DNA damage, redox status change including iron accumulation and periductal fibrosis during CCA genesis induced by administration of Ov and *N*-dinitrosomethylamine (NDMA) in hamsters. Animals were randomly divided into four groups: group I, Ov infection and NDMA administration (ON); group II, Ov infection and NDMA administration and PZ treatment (ONP); the latter 2 groups were similar to group I and II, but group III received additional XN (XON) and group IV received XN plus PZ (XONP). The results showed that high 8-oxodG (a marker of DNA damage) was observed throughout cholangiocarcinogenesis. Moreover, increased expression of CD44v8-10 (a cell surface in regulation of the ROS defense system), whereas decreased expression of phospho-p38$^{MAPK}$ (a major ROS target), was found during the progression of the bile duct cell transformation. In addition, high accumulation of iron and expression of transferrin receptor-1 (TfR-1) in both malignant bile ducts and inflammatory cells were detected. Furthermore, fibrosis also increased with the highest level being on day 180. On the other hand, the groups of XN with or without PZ supplementations showed an effective reduction in all the markers examined, including fibrosis when compared with ON group. In particular, the XONP group in which a

40   significant reduction DNA damage occured, was also found to have iron accumulation and

41   fibrosis compared to the other groups. Our results show that XN administered in combination

42   with PZ could efficiently prevent CCA development and hence provide potential

43   chemopreventive benefits in Ov-induced cholangiocarcinogenesis.

44   **INTRODUCTION**

45        Chronic inflammation induced by liver fluke (*Opisthorchis viverrini*, Ov) infection is the

46   major risk factor for cholangiocarcinoma (CCA) in northeast Thailand. Re-infection of people in

47   endemic areas occurs more likely after praziquantel treatment and frequently leads to periductal

48   fibrosis that governs the pathogenic effects of inflammation and immunity in liver fluke-

49   associated cholangiocarcinogenesis has been recently reviewed (Yongvanit et al. 2012a). Cellular

50   damage caused by reactive oxygen species (ROS) and reactive nitrogen species (RNS) during

51   chronic infection appears to be a key event which is further enhanced by an imbalanced

52   oxidant/anti-oxidant system during reinfections (Yongvanit et al. 2012b). Increase in periductal

53   fibrosis has been shown to be associated with CCA genesis (Prakobwong et al. 2009). After Ov

54   infection, time-dependent periductal fibrosis has been detected with subsequent CCA

55   development (Chamadol et al. 2014; Mairiang et al. 1992).

56        Recently, studies have shown that the expression of CD44 variants form (CD44v) could

57   stabilize xCT (cysteine-glutamate transporter) which promotes cystine uptake and then its

58   conversion to cysteine contributing to glutathione synthesis for ROS defense (Ishimoto et al.

59   2011; Kim et al. 2002). Moreover, Thanee *et al.* showed that an accumulation of CD44v8-10

60   causes suppression of phospho-p38$^{MAPK}$, a major ROS target expression in transforming bile duct

61   cells which is linked to a poor prognosis in CCA patients. In addition, the regulation of redox

62   status in CCA cell lines depends on the expression of CD44v8-10 (Thanee et al. 2016).

63   Therefore, CD44v8-10 plays an important role in redox status regulation via stabilizing xCT in

64    CCA development. During CCA genesis, oxidative stress during chronic inflammation may

65    induce gene related redox status regulation including CD44v to protect bile duct epithelial cells

66    from ROS, hence facilitating CCA genesis.

67            Additionally, iron is an essential nutrient and the most abundant transition metal in human

68    body, where under physiological conditions, it exists in its stable redox states, ferrous ion ($Fe^{2+}$)

69    and ferric ion ($Fe^{3+}$) (Domaille et al. 2008). The essential roles of iron in various biological

70    events, such as oxygen delivery (Wilson & Reeder 2008), electron transport (Rouault & Tong

71    2005), and enzymatic reactions (Aisen et al. 1999; Costas et al. 2004), depend on its redox

72    activity. On the other hand, iron overload causes severe cell damage and organ dysfunction

73    through the abnormal production of ROS (Halliwell & Gutteridge 1992; Xu et al. 2012). Thus,

74    iron plays critically important roles in both healthy and diseased states of the living organisms.

75    The role of iron in carcinogenesis has been shown to be associated with oxidative DNA damage

76    (Wiseman & Halliwell 1996). We have previously reported that transferrin receptor-1 (TfR-1), a

77    cell surface receptor is a candidate molecule for involvement in the increasing of cellular iron

78    uptake in CCA (Jamnongkan et al. 2017). In addition, an increase in TfR-1 has also shown to be

79    responsible for transferrin-mediated iron uptake occurs in breast (Pinnix et al. 2010) and

80    pancreatic cancers (Ryschich et al. 2004).

81            Generally, the gold standard treatment for CCA is surgical resection. However, complete

82    resection is often impossible, and eventually when surgery is achieved, is typically followed by

83    metastasis and/or local recurrence (Khuntikeo et al. 2014; Titapun et al. 2015). The other

84    treatment options such as chemotherapy and radiotherapy have been ineffective for the patients

85    with inoperable tumors. Recently, extensive research has attempted to identify the effective

86    nontoxic nutrients, phytochemical and synthetic pharmacological agents which are believed to

87    have the ability to delay the onset of carcinogenesis process. Curcumin, an anti- inflammatory

88    agent, has been reported in many studies as a potential chemopreventive agent in CCA but the

89  results are quite controversial. So far, it has been shown to inhibit an inflammatory reaction in Ov

90  infected hamsters, but it cannot inhibit Ov-induced CCA in the hamster animal model

91  (Boonjaraspinyo et al. 2009; Pinlaor et al. 2010; Prakobwong et al. 2009). Therefore, other

92  chemopreventive agents need to be identified and explored for their effectiveness in CCA

93  prevention and/or treatment.

94      Xanthohumol (XN) is a principal flavonoid of hop plant (*Humulus lupulus L.*) which has

95  been isolated from hop cones, that are largely used in the brewing industry as a preservative and

96  flavoring agent to add bitterness and aroma to beer (De Keukeleire et al. 1999; Taylor et al.

97  2003). It has been identified as having anti-inflammation, anti-oxidant and cancer

98  chemopreventive activities (Gerhauser 2005).  Moreover, XN has been shown to be associated

99  with induction of apoptosis via increased p21 and p53 expression and decreased surviving levels

100  in a leukemia cell line **(Monteghirfo et al. 2008)**. Additionally, it reduced ROS formation

101  (Hartkorn et al. 2009) and protection against DNA damage (Pinto et al. 2012). Dokduang *et al.*

102  reported that XN effectively suppressed the growth of tumor and induced apoptosis in CCA cells

103  and tumor inoculated mice by which inhibiting STAT3 activation due to suppression of the Akt-

104  NFκB signaling pathway (Dokduang et al. 2016). These data suggested that XN has a potential to

105  become a useful new approach for the chemoprevention and/or treatment of CCA. Additionally,

106  praziquantel (PZ) is well known as a potential drug for liver fluke treatment, which has also been

107  used for removal of Ov. The cure rate of PZ treatment in opisthorchiasis may be as high 100%

108  effective in both humans (Bunnag & Harinasuta 1981; Bunnag et al. 1984) and hamsters

109  (Duenngai et al. 2013). Decreasing levels of liver fibrosis and egg granulomas have been

110  revealed in the liver of patients with blood and liver fluke infections after PZ treatment (Pinlaor

111  et al. 2010).

112      Therefore, this study investigated the effect of XN with or without PZ, on DNA damage,

113  redox status change and periductal fibrosis during CCA genesis in a hamster animal model.

114   **MATERIALS AND METHODS**

115   **Parasite preparation and animal infection**

116        Ov metacercariae were extracted from naturally infected cyprinid fish, which were

117   purchased from the market in Khon Kaen Province, northeast Thailand. The fish were minced

118   and digested with pepsin-HCL, then incubated in shaking water bath at 37ºC for an hour. The

119   digested fish were filtered through the sieves (1,000, 425 and 106 µM respectively) and the

120   filtrate was sedimented with 0.85% saline in a sedimentation jar. Finally, the metacercariae were

121   isolated and identified under a stereomicroscope. Fifty viable active cysts were fed to each of five

122   male Syrian golden hamsters by intragastric intubation.

123   **Xanthohumol preparation**

124        XN was kindly provided by Hopsteiner, Mainberge, Germany. XN -supplemented water

125   was prepared daily as 1 µl of stock 20 mM in 250 µl of distilled-water, yielding a final

126   concentration of 20 µM or 171 mg/B.W./day in the assigned groups. Hamsters were pre-treated

127   with XN more than 14 days before the experiment commenced and treatment was continued until

128   animals were sacrificed at day 60, 90, 120 and 180 post-treatment.

129   ***N*-nitrosodimethylamine preparation and administration**

130        *N*-nitrosodimethylamine (NDMA) (Sigma-Aldrich, St. Louis MO, USA) was diluted in

131   distilled water at 12.5 ppm, and administrated daily to the assigned hamster groups starting on

132   day 30 until day 60 after Ov infection.

133   **Praziquantel preparation**

134        PZ (Sigma-Aldrich, St. Louis MO, USA) was diluted with 2% chemophor, a non-ionic

135   solubilizer and emulsifier. A single dose of 400 mg/kg was administered orally to the assigned

136   treatment groups after day 30 of Ov infection.

137   **Animal groups**

138    The Animal Ethics Committee of Khon Kaen University (AEKKU 23/2555) approved the

139    study protocol. Six- to eight-week-old male Syrian golden hamsters were randomly divided into

140    four groups as followings: group I, Ov infection and NDMA administration (ON); group II, Ov

141    infection and NDMA administration and PZ treatment (ONP); groups III and IV were similar to

142    group I and II, they received 20 µM XN (171 mg/B.W./day) designated as XON and XONP

143    groups, respectively. Hamsters were treated with 50 Ov metacercaria by oral inoculation which

144    was administered with 12.5 ppm of NDMA in water for 30 days and withdrawn thereafter. XN-

145    supplemented water was prepared daily as 1 µl of stock 20 mM in 250 µl of distilled-water. The

146    animals were sacrificed at 60, 90, 120 and 180 days after treatment and hamster liver tissues were

147    collected for further analysis.

148    **General observations**

149    Body and liver weights of each hamster were evaluated at the scarification time. Data

150    were expressed as mean ±SD of liver/body weight. In addition, hamsters in ON, XON, ONP, and

151    XONP groups were used for survival analysis, and the number of surviving hamsters was counted

152    monthly.

153    **Gross observation**

154    Four lobes of the liver (right, left, caudate, and quadrate) were examined for changes in

155    color, appearance of the margins, presence or absence of nodules, and granularity of surfaces,

156    both visually and from photographs taken with a digital camera.

157    **Histological observation by Hematoxylin and Eosin (H&E) staining**

158    Hamster liver tissues were sectioned at a thickness of 4 µm, then fixed in 10% buffered

159    formaldehyde and embedded in paraffin. H&E staining was performed in the sections for

160    histological observation. The sections of liver tissue were deparaffinized in xylene for 3 min for

161    three times to remove the paraffin wax, and then rehydrated in a dilution series of ethanol. The

162    sections were rinsed with tap water, stained with Harr's hematoxylin for 10 min, and then washed

163 with the running tap water for 2 min. Destaining in ethanol containing 1% hydrochloric acid was

164 performed, then washed with running tap water, and stained in saturated lithium carbonate for 3-4

165 sec. The sections mounted on slides were stained with eosin solution after washing with running

166 tap water for 10-20 min. Dehydration of all sections was performed before mounting with

167 permount. Transformation of bile duct cells including normal, hyperplasia, dysplasia and

168 cholangiofibrosis, and cancerous lesions were examined under a light microscope (Axioscope A1,

169 Carl Zeiss, Jena, Germany) at high magnification (x200).

170 **Immunohistochemistry**

171 Sections mounted on slides were deparaffinized in xylene and rehydrated in an ethanol

172 concentration series. Three different methods were used to retrieve antigen from tissue sections;

173 1) for CD44 variant 8-10 staining; 0.5% trypsin-EDTA for 20 min at 37°C incubator, 2) for

174 phospho-p38$^{MAPK}$ and 8-oxodG staining, 0.01 M sodium citrate containing 0.05% Tween 20 (pH

175 6.0) was autoclaved for 10 min at 110°C, and 3) for TfR-1 microwave treatment was performed

176 in 10 mM citrate buffer pH 6.0 at high power for 10 minutes. After that, exposure of 3% $H_2O_2$

177 and 3% bovine serum albumin was performed before further incubation with primary and

178 secondary antibodies, respectively. A Vectastain Elite Kit (Vector Laboratories, Burlingame, CA)

179 and 3,3'-diaminobenzidine was used for detecting the staining signal, and the sections were

180 counterstained with Mayer's hematoxylin. The stained sections were observed under a light

181 microscope at high magnification (x400). The intensity of staining was evaluated semi-

182 quantitatively by the Allred Scoring protocol (Allred et al. 1998).

183 **Prussian blue staining**

184 Prussian blue was used for localization of ferric iron in hamster liver tissues. Hamster

185 liver sections were deparaffinized and rehydrated with graded alcohol. Slides were immediately

186 transferred into a working staining solution (equal volumes of 10% potassium ferrocyanide and

187    10% hydrochloric acid) for 20 minutes at room temperature. Any ferric ions ($Fe^{3+}$) in the tissue

188    combines with the ferrocyanide and result in the formation of a bright blue pigment.

189    Subsequently, slides were rinsed in distilled water, and then counterstained with nuclear-fast red.

190    Finally, sections were dehydrated with stepwise increasing concentrations of ethanol, cleared

191    with xylene and mounted with permount. The stained sections were examined under a light

192    microscope.

193    **Sirius red staining**

194        Sirius red was used for collagen staining. Paraffin sections of each hamster group were

195    dewaxed in xylene and rehydrated with graded alcohol. The sections were stained with

196    haematoxylin and eosin for 8 minutes, washed in distilled water, incubated with 0.1% Sirius red

197    solution dissolved in aqueous saturated picric acid for 1 hour at room temperature, washed in

198    acidified water, dehydrated in xylene, and mounted with mounting medium. The slides were

199    analyzed by light microscope. Collagen, which is the component of fibrosis formation, stained

200    red around the bile duct areas. Therefore, the thickness of periductal fibrosis is stained in red

201    color. The evaluation of staining was adapted using the Batts-Ludwig and IASL for grading

202    fibrosis (Zachary D.G., 2007). Stage 0: no fibrosis; stage 1: mild fibrosis; stage 2: severe fibrosis.

203    **Statistical analysis**

204        Statistical analysis was performed using SPSS software. The difference in general

205    observation results was performed by student's *t*-test (nonparametric: Mann-Whitney test) in two-

206    tailed test. *P*-values of < 0.05 were considered as statistically significant.

207    **RESULTS**

208    **General observations**

209        The liver per body weight of hamster groups either with or without XN and PZ were not

210    significantly different between groups. Moreover, survival curve analysis showed no statistical

211     differences in the time that hamsters survived between each group. However, it seems that the

212     groups with XN treatment had longer survival times either in the presence or absence PZ

213     treatment but this was not statistical significant.

214     **Gross and histological appearances**

215        Gross pathology of the livers revealed smoothness of liver surfaces, although slightly

216     opaque around common bile ducts in all hamsters of both ON and XON groups throughout the

217     experimental period. White granules and small foci were found in the hepatic tissues at day 180

218     after treatment in both ON and XON groups (Figure 1). In addition, the obstruction of gall

219     bladder was seen in ON and XON groups but not in ONP and XONP groups. However, no tumor

220     mass was detected in the liver of all hamsters belonging to the above treatment groups.

221        Histopathological findings revealed no changes in livers and bile ducts in the XN

222     treatment alone, that was similar to untreated group, hence XN was not toxic to liver and bile

223     duct cells. In the ON group, aggregation of inflammatory cells, dilated bile ducts as well as

224     fibrosis was observed at all-time points. Additionally, massive hyperplasia and dysplasia of bile

225     ducts was observed at day 60, 90, 120 and 180. One of the hamsters (1/5, 20%) developed CCA

226     by day 180, whereas the others did not develop CCA. The most severe changes found in the rest

227     of hamsters at day 180 were cholangio-fibrosis.  Interestingly, there was no CCA development

228     observed in the XON group. The most severe pathological changes observed at day 180 in this

229     group was cholangio-fibrosis (4/5, 80%), while only bile duct proliferation and hyperplasia were

230     seen in one of the hamster (1/5, 20%) as shown in Figure 2.  These results indicated that XN

231     could repress the progression of CCA development. Importantly, there was no CCA development

232     in either PZ treated CCA-induced hamster (ONP) or combination with XN treatment (XONP).

233     The most severe pathological changes observed in these groups at day 180 was only bile duct

234     hyperplasia.

235     **Effect of XN with or without PZ supplements on DNA damage**

236    8-oxodG was used as a marker of oxidative stress. A time profile of 8-oxodG formation in

237    the liver of hamsters was evaluated as detected by immunohistochemical staining. The expression

238    of 8-oxodG was observed mainly in the nucleus of bile ducts and inflammatory cells from day 60

239    and reached the highest on day 180 in ON group (Figure 3A). Interestingly, either PZ or XN

240    treatment significantly reduced the accumulation of 8-oxodG starting from day 60 and 120,

241    respectively, when compared with the ON group ($P<0.05$). Moreover, our results showed that the

242    XONP group had significantly and more effectively reduced DNA damage than other groups

243    ($P<0.05$) (Figure 3B).

244    **Effect of XN with or without PZ supplements on redox status**

245    Our result showed that higher CD44v8-10 expression was seen along

246    cholangiocarcinogenesis. The strongest signal of CD44v8-10 was found at day 180 in both

247    dysplasia and malignant area of the bile duct epithelia in ON group (Figure 4A). On the other

248    hand, the highest signal of phospho-p38$^{MAPK}$ which is a downstream target of ROS signaling was

249    seen in the nucleus of the hyperplastic bile duct cells at day 60 and then decreasing of phospho-

250    p38$^{MAPK}$ level was seen along the progression of carcinogenesis in ON group (Figure 4C).

251    Furthermore, both protein levels of CD44v8-10 and phospho-p38$^{MAPK}$ were significantly reduced

252    from day 60 in the ON group treated with either XN or PZ (XON and ONP) ($P<0.05$) (Figure 4B

253    and D). However, no synergistic effect was observed in the XONP group.

254    **Effect of XN with or without PZ supplements on iron accumulation and TfR-1 expression**

255    Prussian blue was used for localization of ferric iron in hamster liver tissues. In the ON

256    group, iron accumulation was observed from 60 days until tumor developed at 180 days (Figure

257    5). The highest accumulation of iron was found at day 180 in both malignant bile duct epithelia

258    and inflammatory cells. In addition, immunohistrochemical staining for TfR-1 protein showed

259    that TfR-1 was localized in bile duct membranes and inflammatory cells (Figure 6A). The highest

260    of its expression was observed in cancerous lesions at day180 in ON group. Interestingly, the

261     reduction of both molecules was seen in XON and ONP groups at day 90 when compared with

262     the ON group. Moreover, our results showed an effective reduction of iron accumulation and

263     TfR-1 expression for the XONP group compared to all other groups. This was especially evident

264     in the expression of TfR-1 in XONP group which was significantly reduced from day 90 ($P<0.05$)

265     (Figure 6B).

266     **The inhibitory effects of XN and PZ on fibrosis**

267     The thickness of periductal fibrosis stained in red color is representative of severe or mild

268     fibrosis. In the ON group, severe fibrosis was seen starting from day 60 until day 180.

269     Additionally, treatment with either XN or PZ (XON and ONP groups) resulted in only mild

270     fibrosis at days 180 and 120, respectively. This was especially so, in the combination treatment or

271     XONP group, where only mild fibrosis was detected from day 60 as shown in Figure 7.

272     **DISCUSSION**

273     At present, the strategies for CCA prevention and treatment are still ineffective and

274     identifying new targets for potential therapeutic prevention of carcinogenesis should be

275     undertaken. A broad-spectrum of cancer chemopreventive agents which act by inhibiting multiple

276     mechanisms for cancer development has been reported (Gerhauser et al. 2002). One of the

277     interesting natural products for cancer prevention is XN. Many studies have indicated that XN

278     can prevent hepatic inflammation and fibrosis during chronic liver diseases as well as the

279     progression of liver cancer (Dorn et al. 2012). Additionally, XN could reduce ROS formation

280     (Hartkorn et al. 2009), protection against DNA damage (Pinto et al. 2012) and regulation of

281     apoptosis and suppression of hepatic stellate cell activation (Yang et al. 2013). These data

282     suggested that the XN has the potential to become a useful new approach for the

283     chemoprevention and/or treatment of CCA.

284       We, therefore, investigated the effect of XN supplement on DNA damage formation in a

285    CCA-induced hamster animal model. The expression of 8-oxodG which is an oxidative stress

286    marker was decreased in XN-treated groups. When used together with PZ (XONP) group it was

287    found to be more effective in reducing DNA damage leading to alteration of redox status and

288    repression of CCA development. This result correlated with our gross and histological

289    observations at day 180 of treatment, which demonstrated that 20% of ON group developed CCA

290    while in the remaing hamsters (80%) only cholangio-fibrosis was found. After XN was

291    supplemented, 20% of hamsters had slow progression of CCA development because only bile

292    duct proliferation and hyperplasia were seen in these groups.  Importantly, there was no CCA

293    development in combination with the PZ treatment (XONP). The most severe pathological

294    changes observed in these groups were only bile duct hyperplasia.

295       We then examined the effect of XN on alteration of redox status. Our results showed that

296    the redox status markers (CD44v8-10 and phospho-p38$^{MAPK}$) were reduced in XN treatment

297    group, and may lead to repression of CCA development via anti-oxidant activity. XN could

298    protect cholangiocytes from oxidative stress during carcinogenesis, consequently, CD44v8-10

299    expression was not induced and phospho-p38$^{MAPK}$ was also decreased.

300       From our previous study, we found that the accumulation of CD44v8-10 led to the

301    suppression of phospho-p38$^{MAPK}$ in transforming bile duct cells. The redox status regulation of

302    CCA cells depends on the expression of CD44v8-10 to contribute the xCT function and is a link

303    to the poor prognosis of patients (Thanee et al. 2016). Importantly, we found that a decrease of

304    CD44v8-10 positive staining was seen during the transformation of bile duct epithelial cells from

305    normal, hyperplasia, and dysplasia in XN treated hamster CCA model. In addition, a high

306    phospho-p38$^{MAPK}$ positive signal staining was observed in both bile duct epithelial cells and

307    surrounding inflammatory cells which was inversely correlated with the transformation of bile

308    duct cells. These results suggested that XN could reduce expression of CD44v8-10 via the

309   possible mechanism of oxidative damage inhibition (reduction of phospho-p38MAPK

310   activation). Furthermore, it has been shown that XN could effectively suppress the growth of

311   tumor and induced apoptosis in CCA cells and tumor inoculated mice (Dokduang et al. 2016).

312   Currently, it has been reported that the oxidative stress could induce Wnt activation (Yoshida &

313   Saya 2014), and then triggered the transcription of CD44 (Ishimoto et al. 2010). Moreover, our

314   group also showed an upregulation of Wnt/β-catenin signaling corresponded with the period of

315   cholangiocarcinogenesis (Yothaisong et al. 2014). Based on this information, the possible

316   mechanism is that the liver fluke infection-induced chronic inflammation causing oxidative stress

317   leads to upregulation of Wnt/β-catenin signaling pathways and consequently increasing of CD44

318   expression, which may drive to CCA carcinogenesis. Hence, an inhibition of oxidative damage

319   using XN could reduce expression of CD44v8-10 possibly via Wnt signaling pathway.

320        We next elucidated the effect of XN supplement on iron accumulation and TfR-1

321   expression. We found both decreasing iron accumulation and TfR-1 expression in bile ducts and

322   inflammatory cells. Iron is an important determinant of ROS generation because an excess of iron

323   can undergo redox reaction and stimulate free radical formation. $H_2O_2$- mediated toxicity was

324   found to be iron mediated. TfR-1 knockdown has been shown to reduce iron uptake by 80% in

325   human hepatoma cell line (Herbison et al. 2009). Moreover, the aberrant expression of TfR-1

326   substantially contributed to the regulation of systemic iron levels and can play key roles in CCA

327   development (Jamnongkan et al. 2017). TfR-1 has been reported to be a major molecule that

328   responded to iron uptake mediated by insulin through hypoxia conditions (Biswas et al. 2013).

329   Andriopoulos et al. found that exposure of cultured cells to sustained low levels of hydrogen

330   peroxide that mimic its release by inflammatory cells lead to up-regulation of TfR-1

331   (Andriopoulos et al. 2007). In steatotic livers, the saturation of β-oxidation by excess free fatty

332   acids will ultimately lead to the generation of hydrogen peroxide, which in turn can be converted

333   to highly reactive hydroxyl radicals in the presence of free iron via Fenton reaction (Videla et al.

334    2003). Indeed, there is strong evidence, from both *in vitro* and *in vivo* studies, that iron overload

335    enhances oxidative stress (Brown et al. 2003; Cornejo et al. 2005; Kadiiska et al. 1995).

336         Sirius red staining was used in each hamster group to assess for levels of collagen which

337    is related to fibrosis. In the revealed a thick and extensive periductal fibrosis was found in the ON

338    group which could be related to Ov-induced fibrosis caused by bile duct lesions that

339    corresponded to the amount of collagen detected. The increased amount of collagen we detected

340    around bile ducts is similar to findings by Prakobwong *et al.* (2009) who also showed that it is

341    dependent on the duration of infection. In addition, we found that XN could reduce fibrosis from

342    day 90 to 180 in another group of hamsters (XON group) (Prakobwong et al. 2009). Hence, XN

343    has the potential to reduce periductal fibrosis in early stages of liver fluke infection as well as

344    efficiently reducing fibrosis in long time treatment. We found that the reduction of fibrosis due to

345    Ov infection was efficiently eliminated by PZ treatment in the ONP group. These results are

346    similar to those of Pinlaor *et al.* who showed the effectiveness of PZ treatment for complete

347    reduction of the fibrosis in liver tissues in order to prevent the progression of the parasite-induced

348    diseases, and CCA development (Pinlaor et al. 2009). Moreover, our study showed that the

349    greatest reduction of fibrosis was in the XONP group compared to all other groups.

350         Praziquantel is well known as a potential drug for Ov treatment and removal of Ov. The

351    cure rate of PZ treatment in opisthorchiasis can be as much as 100% effective in people (Bunnag

352    & Harinasuta 1981; Bunnag et al. 1984) and hamster (Duenngai et al. 2013). Decreasing liver

353    fibrosis and egg granulomas has been revealed in the liver of patients with blood and liver fluke

354    infections after PZ treatment (Pinlaor et al. 2010). In addition, it was demonstrated that

355    promutagenic etheno-DNA and 8-oxodG adducts are most likely to increase the risk of Ov-

356    infected patients to later develop CCA. A relationship between these adduct markers and disease

357    causation is further supported by the protective effect of PZ against DNA damage in human

358    (Dechakhamphu et al. 2010; Thanan et al. 2008). Similarly, this study suggests that CCA

359    development might be suppressed after Ov treatment with PZ. Moreover, we have observed a

360    high efficiency to suppress the progression of CCA in combination treatments between XN and

361    PZ (XONP group). Other studies have indicated that the combination of curcumin (Charoensuk et

362    al. 2011), and *Thunbergia laurifolia* (Wonkchalee et al. 2013) with PZ treatment improved the

363    hepatobiliary system and could retard CCA progression.

364    **CONCLUSIONS**

365         In conclusion, we have demonstrated that PZ can reduce chronic inflammation in

366    combination with XN treatment as well as suppressing oxidative stress possibly via the reduction

367    of DNA damage, iron accumulation, periductal fibrosis and the alterations of intracellular redox

368    lead to delayed CCA development. The proposed mechanism is shown in Figure8. Hence, XN in

369    combination with PZ may prove to be useful chemopreventive agents for CCA prevention.

370    **ACKNOWLEDEMENTS**

371         We would like to acknowledge Prof. Ross H Andrews for editing the MS via Publication

372    Clinic KKU, Thailand.

373    **REFERENCES**

374    Aisen P, Wessling-Resnick M, and Leibold EA. 1999. Iron metabolism. *Curr Opin Chem Biol*

375         3:200-206. 10.1016/S1367-5931(99)80033-7

376    Allred DC, Harvey JM, Berardo M, and Clark GM. 1998. Prognostic and predictive factors in

377         breast cancer by immunohistochemical analysis. *Mod Pathol* 11:155-168.

378    Andriopoulos B, Hegedusch S, Mangin J, Riedel HD, Hebling U, Wang J, Pantopoulos K, and

379         Mueller S. 2007. Sustained hydrogen peroxide induces iron uptake by transferrin

380    receptor-1 independent of the iron regulatory protein/iron-responsive element network. *J*

381    *Biol Chem* 282:20301-20308. 10.1074/jbc.M702463200

382  Biswas S, Tapryal N, Mukherjee R, Kumar R, and Mukhopadhyay CK. 2013. Insulin promotes

383    iron uptake in human hepatic cell by regulating transferrin receptor-1 transcription

384    mediated by hypoxia inducible factor-1. *Biochim Biophys Acta* 1832:293-301.

385    10.1016/j.bbadis.2012.11.003

386  Boonjaraspinyo S, Boonmars T, Aromdee C, Srisawangwong T, Kaewsamut B, Pinlaor S,

387    Yongvanit P, and Puapairoj A. 2009. Turmeric reduces inflammatory cells in hamster

388    opisthorchiasis. *Parasitol Res* 105:1459-1463.

389  Brown KE, Dennery PA, Ridnour LA, Fimmel CJ, Kladney RD, Brunt EM, and Spitz DR. 2003.

390    Effect of iron overload and dietary fat on indices of oxidative stress and hepatic

391    fibrogenesis in rats. *Liver Int* 23:232-242.

392  Bunnag D, and Harinasuta T. 1981. Studies on the chemotherapy of human opisthorchiasis: III.

393    Minimum effective dose of praziquantel. *Southeast Asian J Trop Med Public Health*

394    12:413-417.

395  Bunnag D, Pungpark S, Harinasuta T, Viravan C, Vanijanonta S, Suntharasamai P, Migasena S,

396    Charoenlarp P, Riganti M, and LooAreesuwan S. 1984. Opisthorchis viverrini: clinical

397    experience with praziquantel in Hospital for Tropical Diseases. *Arzneimittelforschung*

398    34:1173-1174.

399  Chamadol N, Pairojkul C, Khuntikeo N, Laopaiboon V, Loilome W, Sithithaworn P, and

400    Yongvanit P. 2014. Histological confirmation of periductal fibrosis from ultrasound

401    diagnosis in cholangiocarcinoma patients. *J Hepatobiliary Pancreat Sci* 21:316-322.

402    10.1002/jhbp.64

403  Charoensuk L, Pinlaor P, Prakobwong S, Hiraku Y, Laothong U, Ruangjirachuporn W, Yongvanit

404    P, and Pinlaor S. 2011. Curcumin induces a nuclear factor-erythroid 2-related factor 2-

405       driven response against oxidative and nitrative stress after praziquantel treatment in liver

406       fluke-infected hamsters. *Int J Parasitol* 41:615-626. 10.1016/j.ijpara.2010.12.011

407  Cornejo P, Varela P, Videla LA, and Fernandez V. 2005. Chronic iron overload enhances

408       inducible nitric oxide synthase expression in rat liver. *Nitric Oxide* 13:54-61.

409       10.1016/j.niox.2005.04.009

410  Costas M, Mehn MP, Jensen MP, and Que L, Jr. 2004. Dioxygen activation at mononuclear

411       nonheme iron active sites: enzymes, models, and intermediates. *Chem Rev* 104:939-986.

412       10.1021/cr020628n

413  De Keukeleire D, De Cooman L, Rong H, Heyerick A, Kalita J, and Milligan SR. 1999.

414       Functional properties of hop polyphenols. *Basic Life Sci* 66:739-760.

415  Dechakhamphu S, Pinlaor S, Sitthithaworn P, Nair J, Bartsch H, and Yongvanit P. 2010. Lipid

416       peroxidation and etheno DNA adducts in white blood cells of liver fluke-infected patients:

417       protection by plasma alpha-tocopherol and praziquantel. *Cancer Epidemiol Biomarkers*

418       *Prev* 19:310-318. 10.1158/1055-9965.EPI-09-0849

419  Dokduang H, Yongvanit P, Namwat N, Pairojkul C, Sangkhamanon S, Yageta MS, Murakami Y,

420       and Loilome W. 2016. Xanthohumol inhibits STAT3 activation pathway leading to growth

421       suppression and apoptosis induction in human cholangiocarcinoma cells. *Oncol Rep*

422       35:2065-2072. 10.3892/or.2016.4584

423  Domaille DW, Que EL, and Chang CJ. 2008. Synthetic fluorescent sensors for studying the cell

424       biology of metals. *Nat Chem Biol* 4:168-175. 10.1038/nchembio.69

425  Dorn C, Heilmann J, and Hellerbrand C. 2012. Protective effect of xanthohumol on toxin-induced

426       liver inflammation and fibrosis. *Int J Clin Exp Pathol* 5:29-36.

427  Duenngai K, Boonmars T, Sithithaworn J, and Sithithaworn P. 2013. Diagnosis of early infection

428       and post chemotherapeutic treatment by copro-DNA detection in experimental

429       opisthorchiasis. *Parasitol Res* 112:271-278. 10.1007/s00436-012-3134-0

430    Gerhauser C. 2005. Beer constituents as potential cancer chemopreventive agents. *Eur J Cancer*
431        41:1941-1954.
432    Gerhauser C, Alt A, Heiss E, Gamal-Eldeen A, Klimo K, Knauft J, Neumann I, Scherf HR, Frank
433        N, Bartsch H, and Becker H. 2002. Cancer chemopreventive activity of Xanthohumol, a
434        natural product derived from hop. *Mol Cancer Ther* 1:959-969.
435    Halliwell B, and Gutteridge JM. 1992. Biologically relevant metal ion-dependent hydroxyl
436        radical generation. An update. *FEBS Lett* 307:108-112.
437    Hartkorn A, Hoffmann F, Ajamieh H, Vogel S, Heilmann J, Gerbes AL, Vollmar AM, and Zahler
438        S. 2009. Antioxidant effects of xanthohumol and functional impact on hepatic ischemia-
439        reperfusion injury. *J Nat Prod* 72:1741-1747. 10.1021/np900230p
440    Herbison CE, Thorstensen K, Chua AC, Graham RM, Leedman P, Olynyk JK, and Trinder D.
441        2009. The role of transferrin receptor 1 and 2 in transferrin-bound iron uptake in human
442        hepatoma cells. *Am J Physiol Cell Physiol* 297:C1567-1575. 10.1152/ajpcell.00649.2008
443    Ishimoto T, Nagano O, Yae T, Tamada M, Motohara T, Oshima H, Oshima M, Ikeda T, Asaba R,
444        Yagi H, Masuko T, Shimizu T, Ishikawa T, Kai K, Takahashi E, Imamura Y, Baba Y,
445        Ohmura M, Suematsu M, Baba H, and Saya H. 2011. CD44 variant regulates redox status
446        in cancer cells by stabilizing the xCT subunit of system xc(-) and thereby promotes tumor
447        growth. *Cancer Cell* 19:387-400. 10.1016/j.ccr.2011.01.038
448    Ishimoto T, Oshima H, Oshima M, Kai K, Torii R, Masuko T, Baba H, Saya H, and Nagano O.
449        2010. CD44+ slow-cycling tumor cell expansion is triggered by cooperative actions of
450        Wnt and prostaglandin E2 in gastric tumorigenesis. *Cancer Sci* 101:673-678.
451        10.1111/j.1349-7006.2009.01430.x
452    Jamnongkan W, Thanan R, Techasen A, Namwat N, Loilome W, Intarawichian P, Titapun A, and
453        Yongvanit P. 2017. Upregulation of transferrin receptor-1 induces cholangiocarcinoma

454        progression via induction of labile iron pool. *Tumour Biol* 39:1010428317717655.

455        10.1177/1010428317717655

456   Kadiiska MB, Burkitt MJ, Xiang QH, and Mason RP. 1995. Iron supplementation generates

457        hydroxyl radical in vivo. An ESR spin-trapping investigation. *J Clin Invest* 96:1653-1657.

458        10.1172/JCI118205

459   Khuntikeo N, Pugkhem A, Titapun A, and Bhudhisawasdi V. 2014. Surgical management of

460        perihilar cholangiocarcinoma: a Khon Kaen experience. *J Hepatobiliary Pancreat Sci*

461        21:521-524. 10.1002/jhbp.74

462   Kim GY, Mercer SE, Ewton DZ, Yan Z, Jin K, and Friedman E. 2002. The stress-activated

463        protein kinases p38 alpha and JNK1 stabilize p21(Cip1) by phosphorylation. *J Biol Chem*

464        277:29792-29802. 10.1074/jbc.M201299200

465   Mairiang E, Elkins DB, Mairiang P, Chaiyakum J, Chamadol N, Loapaiboon V, Posri S,

466        Sithithaworn P, and Haswell-Elkins M. 1992. Relationship between intensity of

467        Opisthorchis viverrini infection and hepatobiliary disease detected by ultrasonography. *J*

468        *Gastroenterol Hepatol* 7:17-21.

469   Monteghirfo S, Tosetti F, Ambrosini C, Stigliani S, Pozzi S, Frassoni F, Fassina G, Soverini S,

470        Albini A, and Ferrari N. 2008. Antileukemia effects of xanthohumol in Bcr/Abl-

471        transformed cells involve nuclear factor-kappaB and p53 modulation. *Mol Cancer Ther*

472        7:2692-2702. 10.1158/1535-7163.MCT-08-0132

473   Pinlaor S, Prakobwong S, Boonmars T, Wongkham C, Pinlaor P, and Hiraku Y. 2009. Effect of

474        praziquantel treatment on the expression of matrix metalloproteinases in relation to tissue

475        resorption during fibrosis in hamsters with acute and chronic Opisthorchis viverrini

476        infection. *Acta Tropica* 111:181-191. 10.1016/j.actatropica.2009.04.011

477    Pinlaor S, Prakobwong S, Hiraku Y, Pinlaor P, Laothong U, and Yongvanit P. 2010. Reduction of

478         periductal fibrosis in liver fluke-infected hamsters after long-term curcumin treatment.

479         *Eur J Pharmacol* 638:134-141. 10.1016/j.ejphar.2010.04.018

480    Pinnix ZK, Miller LD, Wang W, D'Agostino R, Jr., Kute T, Willingham MC, Hatcher H, Tesfay L,

481         Sui G, Di X, Torti SV, and Torti FM. 2010. Ferroportin and iron regulation in breast

482         cancer progression and prognosis. *Sci Transl Med* 2:43ra56. 10.1126/scisignal.3001127

483    Pinto C, Duque AL, Rodriguez-Galdon B, Cestero JJ, and Macias P. 2012. Xanthohumol prevents

484         carbon tetrachloride-induced acute liver injury in rats. *Food Chem Toxicol* 50:3405-3412.

485         10.1016/j.fct.2012.07.035

486    Prakobwong S, Pinlaor S, Yongvanit P, Sithithaworn P, Pairojkul C, and Hiraku Y. 2009. Time

487         profiles of the expression of metalloproteinases, tissue inhibitors of metalloproteases,

488         cytokines and collagens in hamsters infected with Opisthorchis viverrini with special

489         reference to peribiliary fibrosis and liver injury. *Int J Parasitol* 39:825-835.

490         10.1016/j.ijpara.2008.12.002

491    Rouault TA, and Tong WH. 2005. Iron-sulphur cluster biogenesis and mitochondrial iron

492         homeostasis. *Nat Rev Mol Cell Biol* 6:345-351. 10.1038/nrm1620

493    Ryschich E, Huszty G, Knaebel HP, Hartel M, Buchler MW, and Schmidt J. 2004. Transferrin

494         receptor is a marker of malignant phenotype in human pancreatic cancer and in

495         neuroendocrine carcinoma of the pancreas. *Eur J Cancer* 40:1418-1422.

496    Taylor AW, Barofsky E, Kennedy JA, and Deinzer ML. 2003. Hop (Humulus lupulus L.)

497         proanthocyanidins characterized by mass spectrometry, acid catalysis, and gel permeation

498         chromatography. *J Agric Food Chem* 51:4101-4110.

499    Thanan R, Murata M, Pinlaor S, Sithithaworn P, Khuntikeo N, Tangkanakul W, Hiraku Y, Oikawa

500         S, Yongvanit P, and Kawanishi S. 2008. Urinary 8-oxo-7,8-dihydro-2'-deoxyguanosine in

501         patients with parasite infection and effect of antiparasitic drug in relation to

502        cholangiocarcinogenesis. *Cancer Epidemiol Biomarkers Prev* 17:518-524. 10.1158/1055-

503        9965.EPI-07-2717

504  Thanee M, Loilome W, Techasen A, Sugihara E, Okazaki S, Abe S, Ueda S, Masuko T, Namwat

505        N, Khuntikeo N, Titapun A, Pairojkul C, Saya H, and Yongvanit P. 2016. CD44 variant-

506        dependent redox status regulation in liver fluke-associated cholangiocarcinoma: A target

507        for cholangiocarcinoma treatment. *Cancer Sci* 107:991-1000. 10.1111/cas.12967

508  Titapun A, Pugkhem A, Luvira V, Srisuk T, Somintara O, Saeseow OT, Sripanuskul A,

509        Nimboriboonporn A, Thinkhamrop B, and Khuntikeo N. 2015. Outcome of curative

510        resection for perihilar cholangiocarcinoma in Northeast Thailand. *World J Gastrointest*

511        *Oncol* 7:503-512. 10.4251/wjgo.v7.i12.503

512  Videla LA, Fernandez V, Tapia G, and Varela P. 2003. Oxidative stress-mediated hepatotoxicity

513        of iron and copper: role of Kupffer cells. *Biometals* 16:103-111.

514  Wilson MT, and Reeder BJ. 2008. Oxygen-binding haem proteins. *Exp Physiol* 93:128-132.

515        10.1113/expphysiol.2007.039735

516  Wiseman H, and Halliwell B. 1996. Damage to DNA by reactive oxygen and nitrogen species:

517        role in inflammatory disease and progression to cancer. *Biochem J* 313 ( Pt 1):17-29.

518  Wonkchalee N, Boonmars T, Laummaunwai P, Aromdee C, Hahnvajanawong C, Wu Z, Sriraj P,

519        Aukkanimart R, Chamgramol Y, Pairojkul C, Juasook A, and Sudsarn P. 2013. A

520        combination of praziquantel and the traditional medicinal plant Thunbergia laurifolia on

521        Opisthorchis viverrini infection and cholangiocarcinoma in a hamster model. *Parasitol*

522        *Res* 112:4211-4219. 10.1007/s00436-013-3613-y

523  Xu J, Jia Z, Knutson MD, and Leeuwenburgh C. 2012. Impaired iron status in aging research. *Int*

524        *J Mol Sci* 13:2368-2386. 10.3390/ijms13022368

525  Yang M, Li N, Li F, Zhu Q, Liu X, Han Q, Wang Y, Chen Y, Zeng X, Lv Y, Zhang P, Yang C, and

526        Liu Z. 2013. Xanthohumol, a main prenylated chalcone from hops, reduces liver damage

527       and modulates oxidative reaction and apoptosis in hepatitis C virus infected Tupaia

528       belangeri. *Int Immunopharmacol* 16:466-474. 10.1016/j.intimp.2013.04.029

529    Yongvanit P, Pinlaor S, and Bartsch H. 2012a. Oxidative and nitrative DNA damage: key events

530       in opisthorchiasis-induced carcinogenesis. *Parasitol Int* 61:130-135.

531    Yongvanit P, Thanan R, Pinlaor S, Sithithaworn P, Loilome W, Namwat N, Techasen A, and

532       Dechakhamphu S. 2012b. Increased expression of TLR-2, COX-2, and SOD-2 genes in

533       the peripheral blood leukocytes of opisthorchiasis patients induced by Opisthorchis

534       viverrini antigen. *Parasitol Res* 110:1969-1977. 10.1007/s00436-011-2725-5

535    Yoshida GJ, and Saya H. 2014. Inversed relationship between CD44 variant and c-Myc due to

536       oxidative stress-induced canonical Wnt activation. *Biochem Biophys Res Commun*

537       443:622-627. 10.1016/j.bbrc.2013.12.016

538    Yothaisong S, Thanee M, Namwat N, Yongvanit P, Boonmars T, Puapairoj A, and Loilome W.

539       2014. Opisthorchis viverrini infection activates the PI3K/ AKT/PTEN and Wnt/beta-

540       catenin signaling pathways in a Cholangiocarcinogenesis model. *Asian Pac J Cancer*

541       *Prev* 15:10463-10468.

# Figure 1

Gross findings of hamster liver tissues.

Photographs are representative at days 60, 90, 120, and 180 in four groups including the control (ON), presence of xanthohumol (XON), presence of praziquantel (ONP) and presence of xanthohumol and praziquantel (XONP) groups. Results show the obstruction of gall bladder in ON and XON groups at 60, 90, 120, and 180 days but not in the ONP and XONP groups. Additionally, white granules were observed at day 180 in ON and XON groups. Arrowheads indicate white granules and small foci.
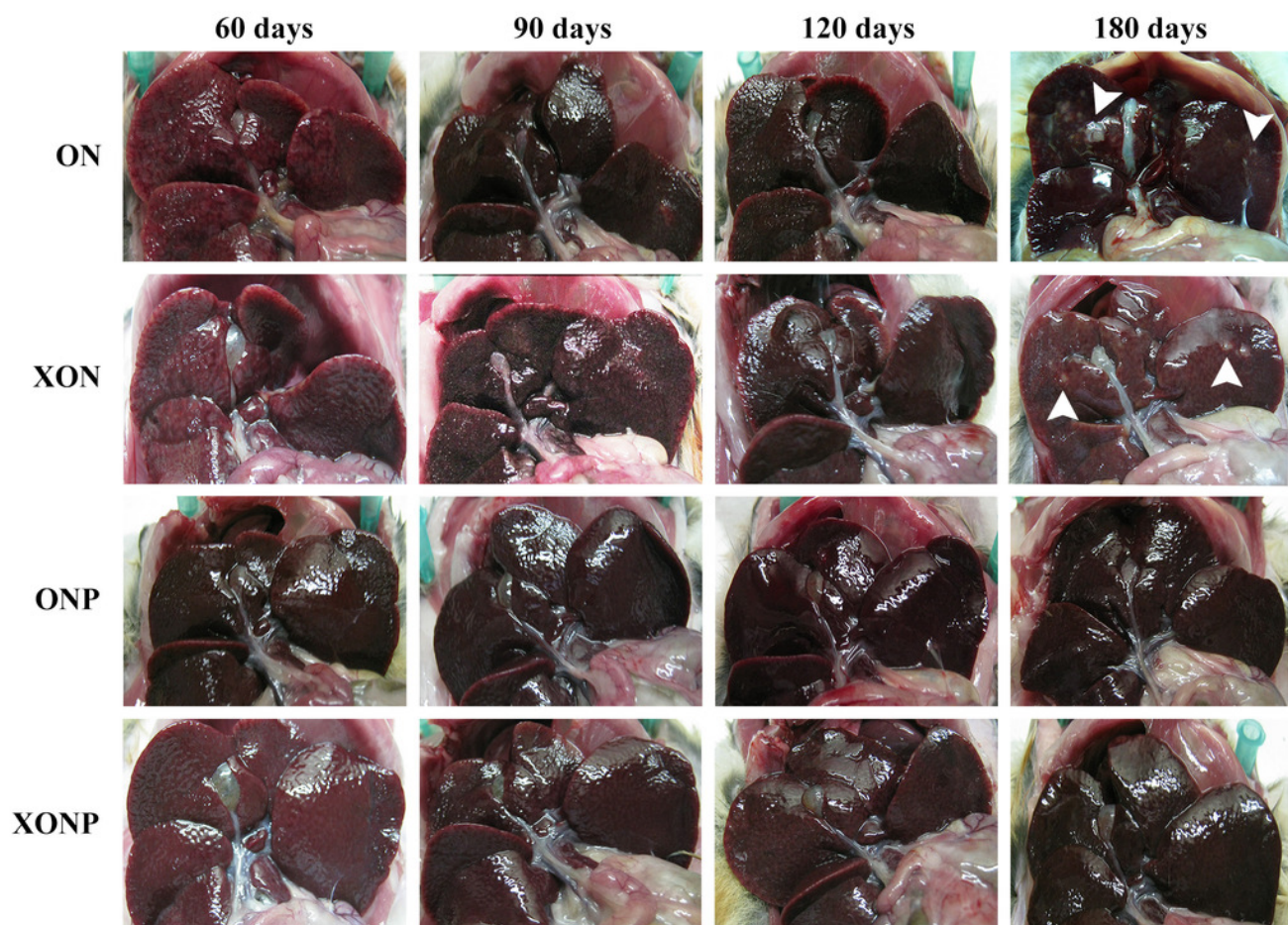
# Figure 2

Histological changes in Ov-induced CCA hamsters with the control (ON), presence of xanthohumol (XON), presence of praziquantel (ONP) and presence of xanthohumol and praziquantel (XONP) groups.

Circles represent: Ov, *O. viverrini*; BD, bile duct; IF, inflammation area; HD, hyperplasia bile duct; PD, proliferative bile duct.
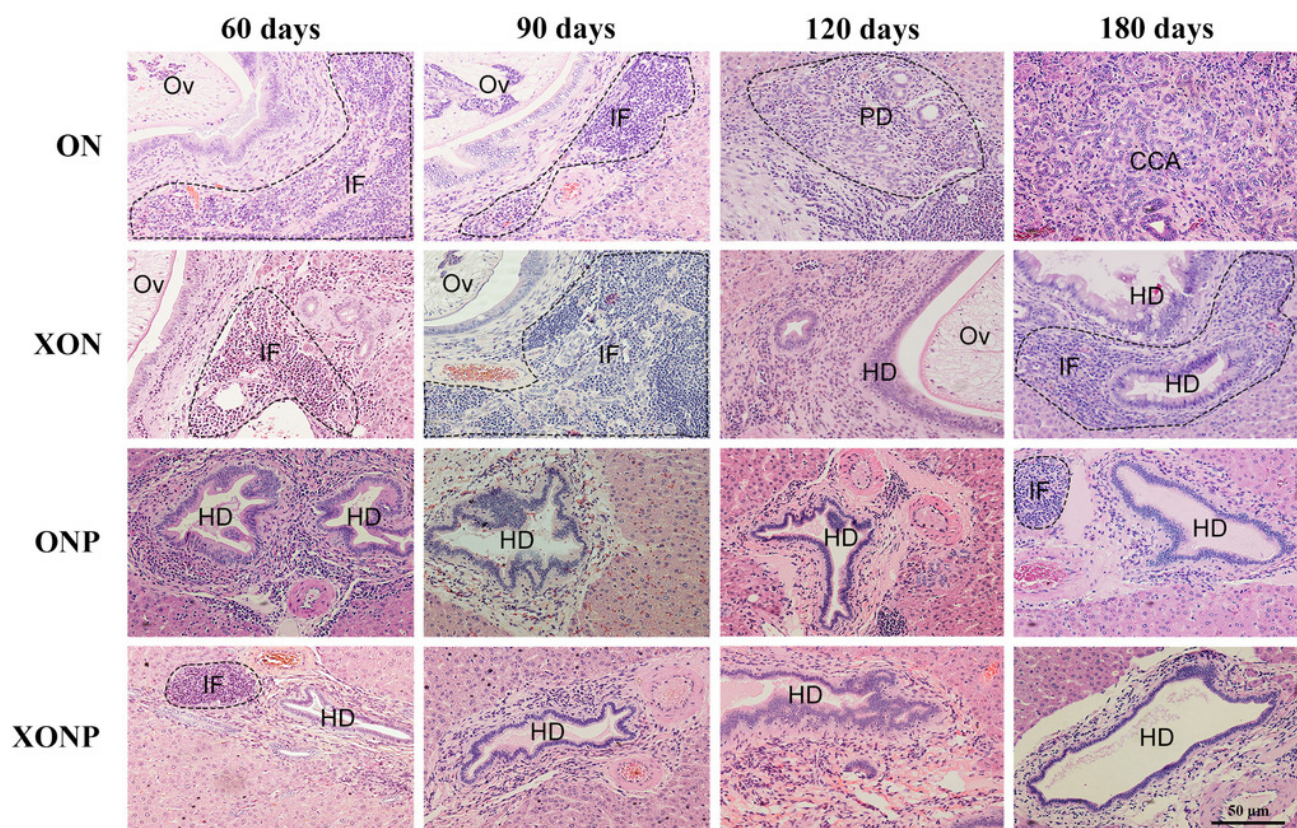
# Figure 3

Immunostaining of 8-oxodG in CCA genesis hamsters.

Localization of 8-oxodG in the control (ON), presence of xanthohumol (XON), presence of praziquantel (ONP) and presence of xanthohumol and praziquantel (XONP) groups (A). Bar graph comparisons of frequency and intensity using Allred score in each group of hamster liver (B). *P < 0.05 compared to ON group.

**A**

|  | 60 days | 90 days | 120 days | 180 days |

**ON**

**XON**

**ONP**

**XONP**

50 μm

**B**
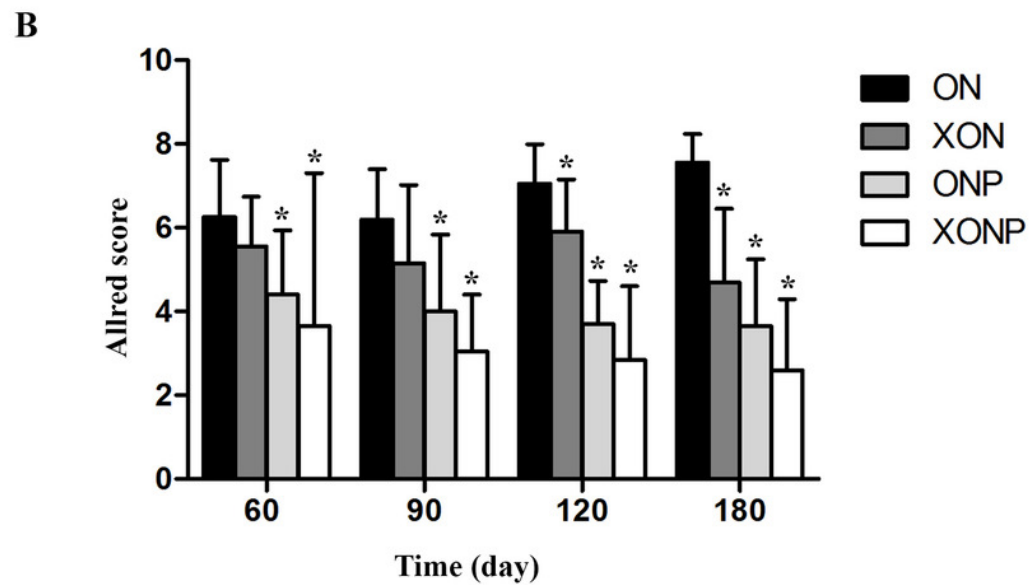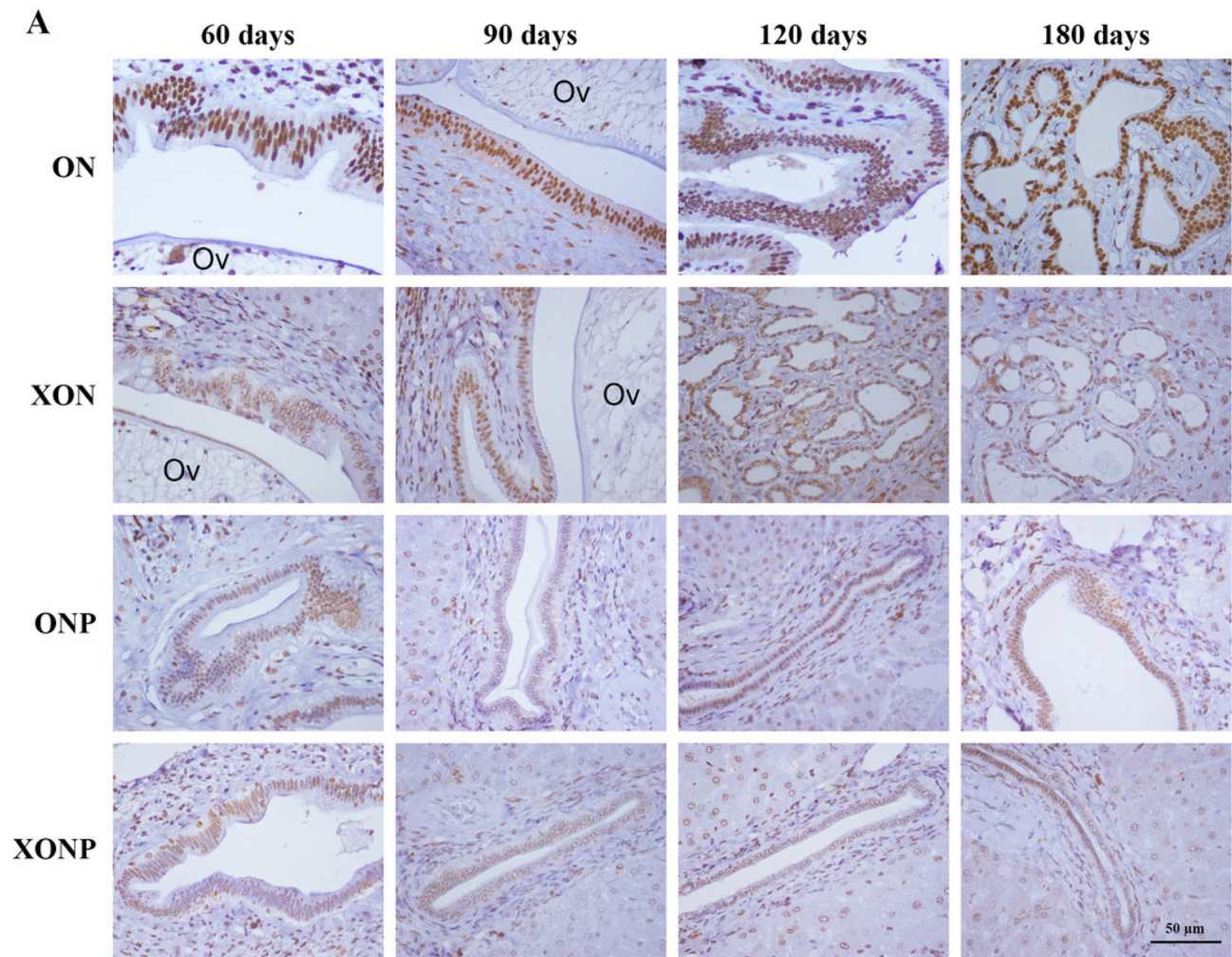
# Figure 4

Immunostaining of CD44v8-10; cancer stem-like cells (A) and phospho-p38$^{MAPK}$; downstream of ROS signaling (C) in CCA genesis in hamsters.

Photographs are representative of the control (ON), presence of xanthohumol (XON), presence of praziquantel (ONP) and presence of xanthohumol and praziquantel (XONP) groups. Bar graph comparisons of frequency and intensity using Allred score in each group of hamster liver (B and D). *P < 0.05 compared to ON group.

**A**

|  | 60 days | 90 days | 120 days | 180 days |
|---|---|---|---|---|
| ON | | | | |
| XON | | | | |
| ONP | | | | |
| XONP | | | | |

**B**

**C**

|  | 60 days | 90 days | 120 days | 180 days |
|---|---|---|---|---|
| ON | | | | |
| XON | | | | |
| ONP | | | | |
| XONP | | | | |

**D**
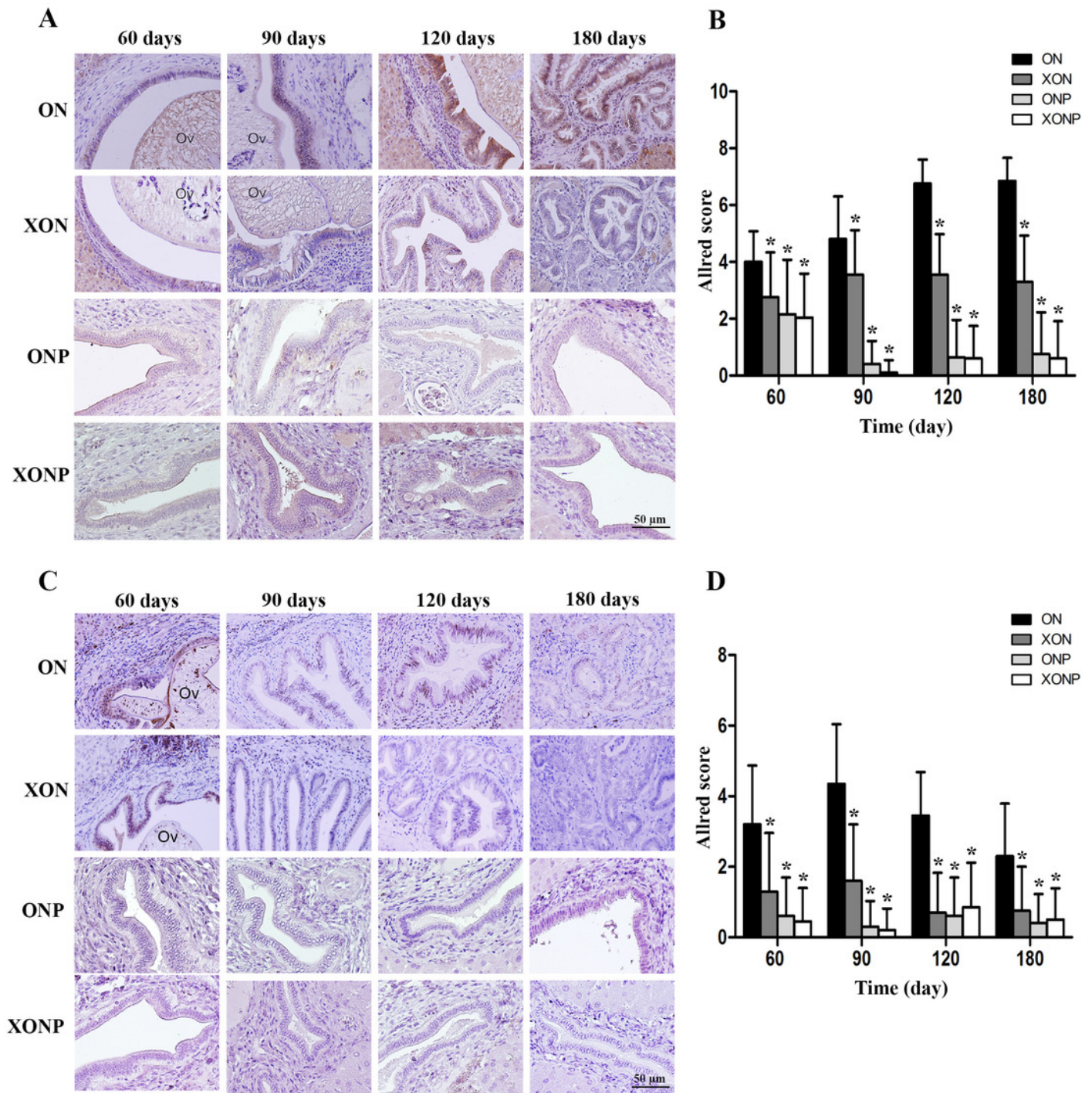
# Figure 5

Prussian blue staining of iron in CCA genesis hamsters.

Photographs are representative of the control (ON), presence of xanthohumol (XON), presence of praziquantel (ONP) and presence of xanthohumol and praziquantel (XONP) groups.
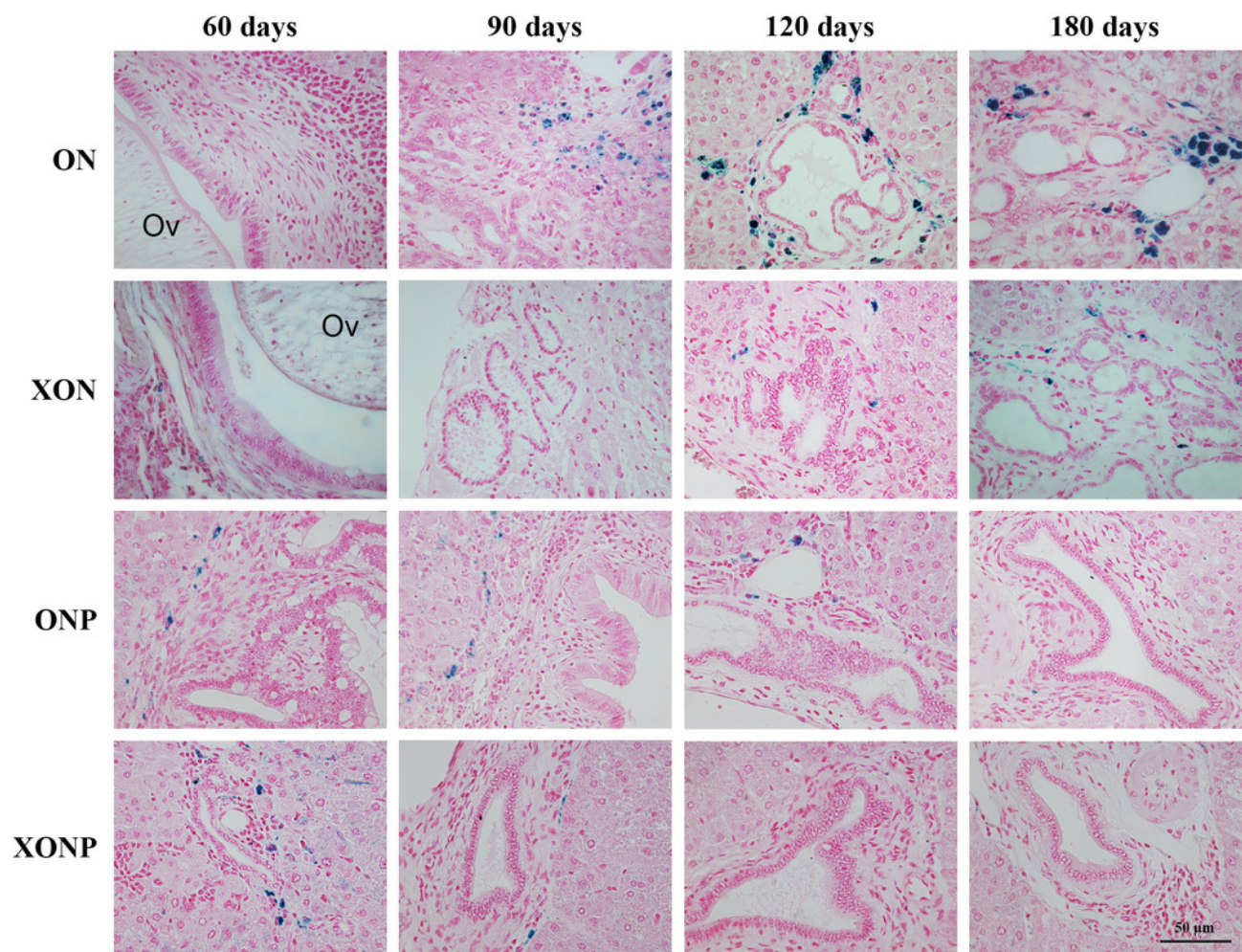
# Figure 6

Immunohistochemistry for in CCA genesis hamsters.

Photographs are representative of the control (ON), presence of xanthohumol (XON), presence of praziquantel (ONP) and presence of xanthohumol and praziquantel (XONP) groups (A). Bar graph comparisons of frequency and intensity using Allred score in each group of hamster liver (B). *$P < 0.05$ compared to ON group.
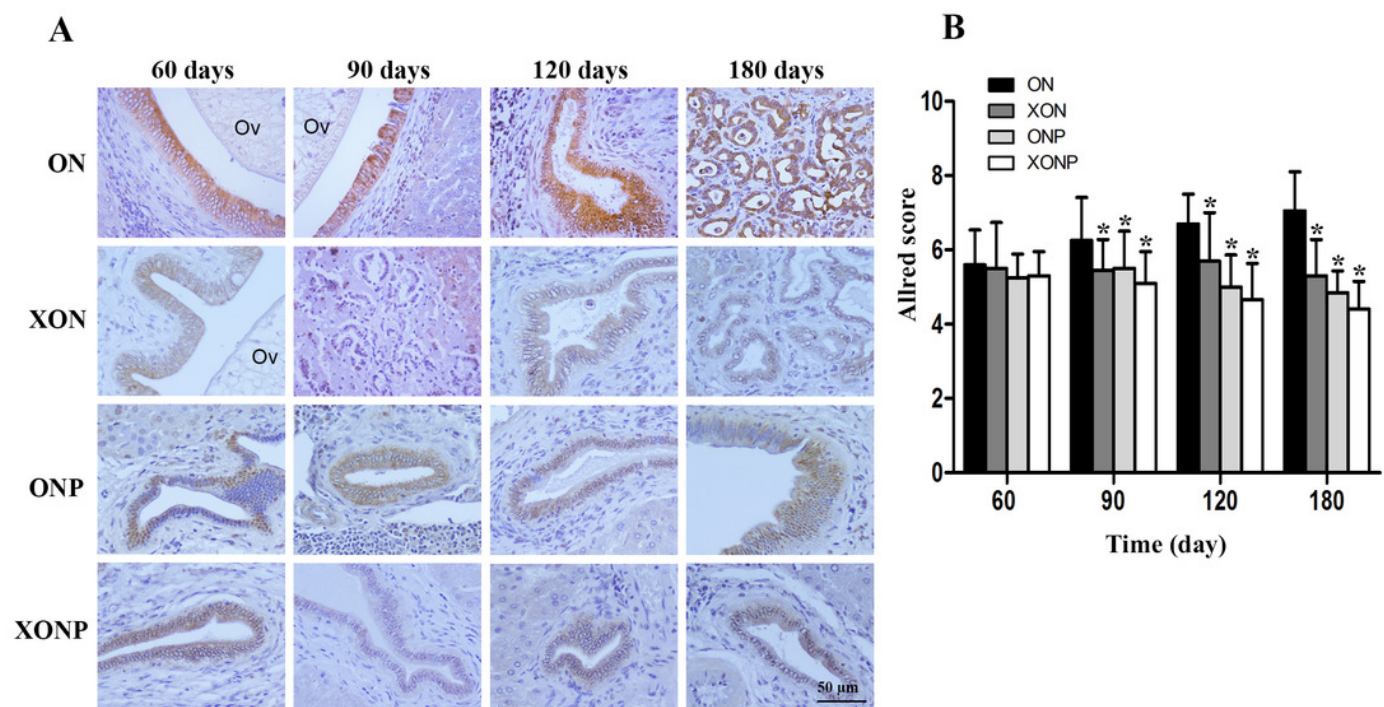
# Figure 7

Sirius red staining for collagen in CCA genesis hamsters with the control (ON), presence of xanthohumol (XON), presence of praziquantel (ONP) and presence of xanthohumol and praziquantel (XONP) groups.

Thickness of red color represents fibrosis area.
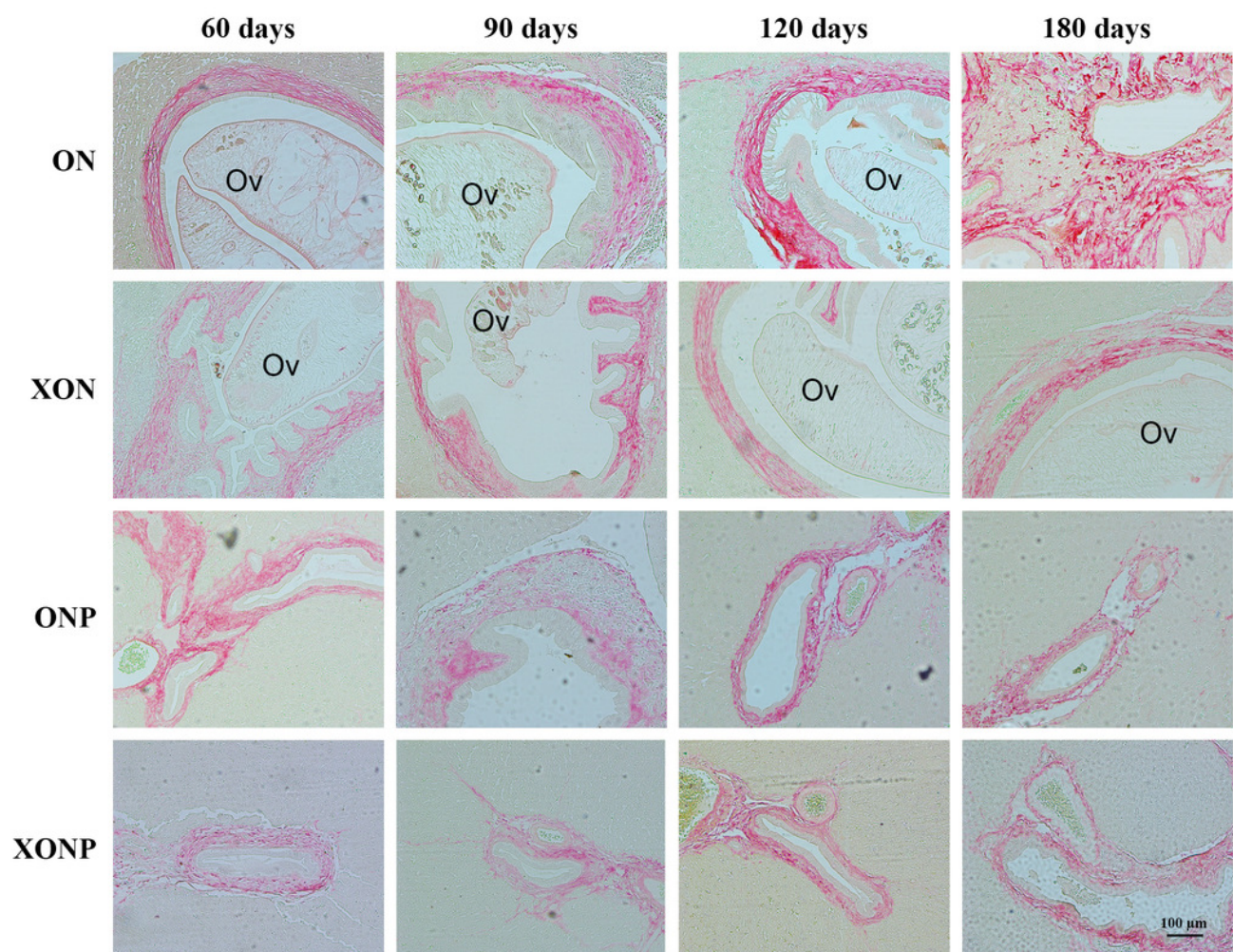
A possible chemopreventive effect of xanthohumol in combination with praziquantel.

Xanthohumol in combination with praziquantel could serve as potential anti-inflammation, anti-oxidant and antifibrotic agents in liver fluke-induced inflammation in relation to CCA development. Legend: ↓, regulate; ⊥, inhibit.